AD-769 962

SOLID STATE MATERIALS AND DEVICES

Fredrik A. Lindholm, et al

Florida University

Prepared for:

Advanced Research Projects Agency
Air Force Cambridge Research Laboratories

10 April 1973

DISTRIBUTED BY:

NTIS

National Technical Information Service
U. S. DEPARTMENT OF COMMERCE
5285 Port Royal Road, Springfield Va. 22151

Unclassified

Security Classification

AD 769962

DOCUMENT CONTROL DATA - R&D

(Security classification of title, body of abstract and indexing annotation must be entered when the overall report is classified)

1. ORIGINATING ACTIVITY *(Corporate author)*

University of Florida
Engineering and Industrial Experiment Station
Gainesville, Florida 32601

2a. REPORT SECURITY CLASSIFICATION

Unclassified

2b. GROUP

3. REPORT TITLE

SOLID STATE MATERIALS AND DEVICES

4. DESCRIPTIVE NOTES *(Type of report and inclusive dates)*

Scientific Interim

5. AUTHOR(S) *(First name, middle initial, last name)*

Fredrik A. Lindholm
Arthur J. Brodersen
Eugene R. Chenette
Sheng S. Li
C. T. Sah

6. REPORT DATE	7a. TOTAL NO. OF PAGES	7b. NO. OF REFS
10 April 1973	234	22

8a. CONTRACT OR GRANT NO.	9a. ORIGINATOR'S REPORT NUMBER(S)
F-19628-72-C-0368	Scientific Report No. 1
b. PROJECT, TASK, WORK UNIT NOS.	
c. DOD ELEMENT	9b. OTHER REPORT NO(S) *(Any other numbers that may be assigned this report)*
d. DOD SUBELEMENT	AFCRL-TR-73-0529

10. DISTRIBUTION STATEMENT

A - Approved for public release; distribution unlimited

11. SUPPLEMENTARY NOTES	12. SPONSORING MILITARY ACTIVITY
This research was supported by Advanced Research Projects Agency	Air Force Cambridge Research Laboratories (LQ) L. G. Hanscom Field Bedford, Massachusetts 01730

13. ABSTRACT

Generalized hydrodynamic carrier transport equations for semiconductors are derived for materials having comparable scattering and generation-recombination-trapping-tunneling rates. Band-to-band radiative recombination in n-type gallium arsenide doped with oxygen is measured by photomagnetoelectric and photoconductive methods at 20.8°K and 4.2°K. These same methods of measurement are used to reveal the dependence of excess carrier lifetimes on photoinjected carrier densities in gallium arsenide doped with chromium. The existence of an interfacial layer is revealed and its effects characterized for a gold-gallium arsenide Schottky diode by measurement of the current-voltage characteristics at very low reverse bias.

Reproduced by
NATIONAL TECHNICAL
INFORMATION SERVICE
U S Department of Commerce
Springfield VA 22151

ia

DD FORM 1 NOV 65 1473

Unclassified

Security Classification

14. KEY WORDS	LINK A		LINK B		LINK C	
	ROLE	WT	ROLE	WT	ROLE	WT
semiconductors						
carrier transport						
gallium arsenide						
diodes						
carrier lifetime						

AFCRL-TR-73-0529

SOLID STATE MATERIALS AND DEVICES

by

Fredrik A. Lindholm, Arthur J. Brodersen, Eugene R. Chenette,
Sheng S. Li and C. T. Sah

Electrical Engineering Department
College of Engineering
University of Florida
Gainesville, Florida 32601

Contract No. F 19628-72-C-0368

Project No. 1060

Scientific Report No. 1
10 April 1973

Contract Monitor
Andrew C. Yang
Solid State Sciences Laboratory

Approved for public release; distribution unlimited.

Sponsored by

Advanced Research Projects Agency
ARPA Order No. 1060

Monitored by

AIR FORCE CAMBRIDGE RESEARCH LABORATORIES
AIR FORCE SYSTEMS COMMAND
UNITED STATES AIR FORCE
BEDFORD, MASSACHUSETTS 01730

ic

ARPA Order No. 1060

Program Code No. 2D1

Contractor: University of Florida

Effective Date of Contract: 1 September 1972

Contract No. F19628-72-C-0368

Principal Investigator and Phone No.
Dr. Fredrik A. Lindholm/904 392-0904

Project Scientist and Phone No.
Dr. Andrew C. Yang/617 861-2225

Contract Expiration Date: 31 August 1973

Qualified requestors may obtain additional copies from the Defense Documentation Center. All others should apply to the National Technical Information Service.

ID

ABSTRACT

Generalized hydrodynamic carrier transport equations for semiconductors are derived for materials having comparable scattering and generation-recombination-trapping-tunneling rates. Band-to-band radiative recombination in n-type gallium arsenide doped with oxygen is measured by photomagnetoelectric and photoconductive methods at 20.8°K and 4.2°K. These same methods of measurement are used to reveal the dependence of excess carrier lifetimes on photoinjected carrier densities in gallium arsenide doped with chromium. The existence of an interfacial layer is revealed and its effects characterized for a gold-gallium arsenide Schottky diode by measurement of the current-voltage characteristics at very low reverse bias.

SUMMARY

This report describes technical findings concerning properties of semiconductors that bear on the design of photodetectors and on the modeling of various semiconductor devices.

The conventional thermodynamics transport equations used in the analysis of the electrical characteristics of semiconductor devices require modifications when the rate of recombination-generation-trapping-tunneling events becomes comparable with the rate of scattering events. These modifications may become important in such basic problems as describing the transport of minority carriers across the thin base region of a high-frequency transistor, and particularly in the analysis of devices made of compound semiconductors with high mobility and low lifetime. Further modifications in the equations traditionally used in analysis arise when the signal frequency becomes comparable to the collision frequency. In the study described here, generalized hydrodynamic transport equations are derived by extending the moment method to include the moment equation of the collision free path, which itself is generalized to include both scattering and generation-recombination-trapping-tunneling events. When the signal frequency becomes comparable with the reciprocal average collision relaxation time, the electron current equation derived in this way contains a new inductive term, which appears as an inductor in the describing circuit model.

We describe photoinjected carrier recombination processes in gallium arsenide doped with oxygen at 4.2°K and 20.8°K by photomagnetoelectric and photoconductive measurements made under large-injection conditions. By assuming direct band-to-band radiative recombination, we derive an expression for the photomagnetoelectric short-circuit current in terms of the radiative capture rate and the photoconductance. From this, the capture rates are determined directly from the data, which shows good agreement with that computed using the direct radiative recombination model due to Hall.

For gallium arsenide doped with chromium, photomagnetoelectric and photoconductive measurements at 300°K and 80°K are used to investigate the dependence of excess carrier lifetimes on the photoinjected carrier densities.

The study reveals three distinct injection ranges spanning five orders of magnitude change in photoconductance. The lifetimes remain constant in both the low and high injection ranges, but show dependence on injection in the intermediate range. We advance a theory to explain these observations.

Measurement of the current-voltage characteristics at very low reverse bias is used to reveal the existence of an interfacial layer in a gold-gallium arsenide Schottky diode. The effect of the interfacial layer is characterized in terms of a voltage-dividing factor.

TABLE OF CONTENTS

I. Introduction

The research program sponsored by this contract involves studies in several different problem areas:

(a) the further development of Schottky-barrier photodiodes made with a new mask structure proposed recently at the University of Florida, and collateral studies concerned with material properties relevant to photodetection;

(b) inferences from the noise spectrum measured in semiconductor devices, including irradiated junction field-effect transistors;

(c) modeling of semiconductor devices for computer-determined design including characterization for exposure to radiation environments; and

(d) study of the potential of carrier-domain devices in electronic system applications.

The content of this report deals mainly with material properties pertinent to the design of photodetectors and the modeling of semiconductor devices.

II. Transport in Semiconductors with Low Scattering Rate and at High Frequencies (C. T. Sah and F. A. Lindholm)

Conventional hydrodynamic transport equations used in the analysis of the electrical characteristics of semiconductor devices require modifications when the number of recombination-generation-trapping-tunneling events becomes comparable with the number of scattering events. Examples are the transport of the minority carriers across the thin base region of a microwave transistor which are injected at the emitter edge with a density distribution function $f(\vec{r},\vec{v},t)$ and devices made of the high mobility and low lifetime compound semiconductors. Further modifications arise if the signal frequency becomes comparable to the collision frequency. Then an inductive delay of the conduction current due to collision would be expected, such as that in the cyclotron resonance experiments, which is neglected in the conventional device analysis. The flux method was proposed as an exact approach to this type of problem [1] but was shown [2] to be based on simplifying and unrealistic assumptions.

The generalized Boltzmann equation is employed here whose collision terms include both the scattering events (initial and final states of electron are in one band) and generation-recombination-trapping-tunneling events (the initial or final state is either a bound or band state in another band) [3]. This one-particle Boltzmann equation can be derived from the N-particle Louiville equation and is given by

$$df/dt = \partial f/\partial t + \vec{k}\cdot\nabla_k f + \vec{v}\cdot\nabla_r f = (df/dt)_c = (df/dt)_s + (df/dt)_{grtt} \qquad (1)$$

Here $f=f(\vec{r},\vec{k},t)$ is the one-particle distribution function for electrons and $f(\vec{r},\vec{k},t)dVdV_k$ is the number of electrons in the macroscopic volumes $dV=dxdydz$ in position space and $dV_k=2dk_x dk_y dk_z/(2\pi)^3$ in wave number of $\vec{k}$ space. $\vec{k}$ labels the Bloch electron states of the unperturbed crystal and is limited to one band (conduction or valence band) and to the reduced Brillouin Zone since terms from interband and band-bound transitions due to generation-recombination-trapping or tunneling processes are already included in the

collision term $(df/dt)_{grtt}$. The force equation of the Bloch electron is given by $\vec{F}=\hbar\dot{\vec{k}}=-q(\vec{E}+\vec{v}x\vec{B})$ where $\vec{E}$ and $\vec{B}$ are the electric and magnetic fields and $\vec{v}=\nabla_k E_k/\hbar$ is the group velocity. $E_k=E(\vec{k})$ is the one electron energy-wave number relationship of the unperturbed crystal.

The collision term, $(df/dt)_c$, in (1) is separated into two terms: the scattering term $(df/dt)_s$ due to the various scattering events whose initial and final states are Bloch states and the generation-recombination-trapping-tunneling (grtt) term $(df/dt)_{grtt}$. Usually, $(df/dt)_{grtt} \ll (df/dt)_s$ is assumed so that the former is dropped in the mobility and diffusivity calculations. This assumption will not be made here. It becomes invalid in materials containing high concentrations of imperfection centers.

A relaxation time shall be assumed to exist for the scattering events which can be justified in certain cases [4] so that $(df/dt)_s=-(f-f_o)/\tau_s$ where $f_o=1/[1+\exp(E_k-E_F)/k_BT]$ is the equilibrium or Fermi-Dirac distribution function and τ_s is the scattering relaxation time. An operational relaxation time for the generation-recombination-trapping-tunneling events shall be defined by $(df/dt)_{grtt}=-(f-f_o)/\tau_{grtt}$ in order to put the solutions of the Boltzmann equation in a form which can be readily compared with the conventional solutions where the grtt processes are neglected. An estimate can readily be made for τ_{grtt} from the capture and emission of electrons at the bound states of an imperfection center, giving $\tau_{grtt}^{-1} \simeq \Sigma(t)P_{kt} < e_n = \Sigma\Sigma(k,t)P_{kt}$. Here P_{kt} is the thermal equilibrium transition probability per unit time from the first order time dependent perturbation theory for the emission transition from a bound state t to a band state $\vec{k}$. Those scattering events at this imperfection center (band-band transition) are implicitly included in τ_s. A numerical estimate can be made for the thermal or phonon-assisted capture and emission events since $e_n=e_n^t=\sigma_n\theta_n N_C\exp[(E_T-E_C)/k_BT] \simeq 10^{12}\exp[(E_T-E_C)/k_BT]$ sec^{-1} where we let the emission-capture cross section be $\sigma_n \simeq 10^{-14}$ cm^2, the thermal velocity $\theta_n \simeq 10^7$ cm/sec and the effective density of state $N_C \simeq 10^{19}$/cm^3. Thus, for a bound state energy E_T near the band edge E_C, $\tau_{grtt} > e_n^{-1} \simeq 10^{-12}$ sec which becomes comparable with $\tau_s \simeq 10^{-12}$ sec for a mobility of about 1500 cm^2/V-s.

Using these relaxation times, the collision term can be written as $(df/dt)_c=-(f-f_o)/\tau$ where the total collision relaxation time is given by $\tau=\tau_s\tau_{grtt}/(\tau_s+\tau_{grtt})$. The Boltzmann equation, (1), is then reduced to the conventional form which may be multiplied by a general function $\phi(r,v,t)$ and

integrated over the reduced Brillouin Zone to give the solid state analog of the moment or hydrodynamical equations and conservation theorems which are well known in gas dynamics and plasma physics. [5] For $\phi(r,v,t)=1$, we have the continuity equation for electrons (or holes)

$$\partial n/\partial t + \nabla\cdot(\vec{j}_N/q) = g_N \tag{2}$$

where $n=\int f dV_k$, $\vec{j}_N=-q\int v f dV_k$ and $g_N=\int(df/dt)_{grtt} dV_k$. For $\phi(r,v,t)=\vec{v}$ or E_k, the momentum or energy conservation theorems are obtained. In order to get the current equations, we let $\phi=\lambda_\alpha\equiv v_\alpha\tau$ where λ_α is the α-th component of the free path. Then, integrating ϕf over the reduced Brillouin Zone and using (1) and $(df/dt)_c=-(f-f_o)/\tau$ to get τ, we have

$$(\partial/\partial t)(n<\lambda_\alpha>) + D\nabla_\alpha n + \mu n E_\alpha = j_{N\alpha}/q \tag{3}$$

where α=x, y or z. The diffusivity and mobility are given by $D=\int v_\alpha\tau\vec{v}\cdot\nabla_r f dV_k/\int\nabla_\alpha f dV_k\simeq<v_\alpha^2\tau>$ and $\mu=(q/\hbar)<\nabla_{k_\alpha}\lambda_\alpha>\simeq(q/m_\mu)<\tau E_k>/<E_k>$ where the conventional forms after the approximate signs are obtained if it is assumed that $f(\vec{r},\vec{k},t)=f(\vec{k}.t)g(\vec{r})$ such as in the Maxwellian approximation. The average is defined by $<A>=\int A f dV_k/\int f dV_k$. (3) can be readily extended to anisotropic cases by generalizing λ, D and μ to 3x3 matrices.

The new time dependent term in (3), $(\partial/\partial t)(n<\lambda_\alpha>)$, although well known in contributing to line width and energy loss in cyclotron resonance and infrared carrier absorption experiments, has been treated commonly using a particle model [6] which can be justified from (3) only if τ is independent of electron velocity or k. It is completely neglected in applying (3) to device analysis.

Eq. (3) can be simplified if the time dependence of f can be factored out as $f(\vec{r},\vec{k},t)=f(\vec{k})g(\vec{r})h(t)$. A sufficient condition for this factorization is the small-signal condition. For this case and using $j_N=-q\int v_\alpha f dV_k$ for the time derivative term, (3) becomes

$$[1 + \bar{\tau}(\partial/\partial t)]j_{N\alpha} = q\mu n E_\alpha + qD\nabla_\alpha n \tag{4}$$

where $\bar{\tau}=<v_\alpha\tau>/<v_\alpha>$. This result indicates an inductive delay of the conduction current j_N due to the collision events. It gives rise to an inductance, $L_n=\bar{\tau}_n/q\mu_n n$, in series with $\sigma_n=q\mu_n n$ in the electron current line and $L_p=\bar{\tau}_p/q\mu_p p$ in series with $\sigma_p=q\mu_p p$ in the hole current line of the circuit

model of carrier transport. [3]. The delay becomes important when signal frequency becomes comparable to $1/2\pi\tau \simeq 10^{12}/2\pi$ Hz and gives rise to the resonance and line width effect in cyclotron resonance experiments.

REFERENCES

1. McKelvey, J. P., Longini, R. L. and Brody, T. P., "Alternative Approach to the Solution of Added Carrier Transport Problems in Semiconductors," Physical Review 1961, 123, 51.
2. Shockley, W., "Diffusion and Drift of Minority Carriers in Semiconductors for Comparable Capture and Scattering Mean Free Paths," Physical Review 1962, 125, 1570.
3. Sah, C. T., "Equivalent Circuit Models in Semiconductor Transport for Thermal, Optical, Auger-Impact and Tunneling Recombination-Generation-Trapping Processes," Physica Status Solidi a, 1971, 7, 541.
4. Herring, C., "Transport Properties of a Many-Valley Semiconductor," Bell. Sys. Tech. J. 1955, XXXIV, 237.
5. Chapman, S. and Cowling, T. G., "The Mathematical Theory of Non-uniform Gases," (Cambridge University Press, 1960) Section 3.12, 48;
   Huang, K, "Statistical Mechanics,"(Wiley, 1965) section 5.2, 95;
   Reif, K., "Fundamentals of Statistical and Thermal Physics," (McGraw-Hill, 1965) section 14.4 and 14.5, 525, 529;
   Liboff, R. L., "Introduction to the Theory of Kinetic Equations," (Wiley, 1969), section 4.4, 231; and
   Harris, S., "An Introduction to the Theory of Boltzmann Equation," (Holt, Rinehart and Winston, Inc. 1971), section 2-4, 26.
6. Smith, R. A., "Semiconductors," (Cambridge University Press, 1959), sections 7.6 and 7.8, 216, 223; and
   Kittel, C., "Introduction to Solid State Physics," (Wiley, 1967), 319.

III. Radiative Recombination in O_2-Doped n-Type GaAs at Low Temperatures

(Sheng S. Li and Chern I. Huang)

I. Introduction

Studies of the recombination mechanisms in undoped GaAs single crystals in the temperature ranges from 77°K to 300°K have been made previously by Braunstein,[1] Mayburg,[2] Kinsel and Kudman[3] respectively. From the carrier lifetime data, these authors have claimed that the direct band to band radiative transition process is responsible for the recombination of electrons and holes in the gallium-arsenide crystals.

In this paper we report our recent study of the photoinjected carrier recombination processes in O -doped GaAs at 4.2°K and 20.8°K by using photomagnetoelectric (PME) and photoconductive (PC) methods under large injection conditions. By assuming direct band to band radiative recombination, an expression for the PME short circuit current is derived in terms of the radiative capture rate and the photoconductance. From this the capture rates can be determined directly from the PME and PC measurements. The results are compared with the Hall's direct radiative recombination model[4] of the host crystal.

II. Theory

(A) Band to band radiative recombination in the host crystal

The theory of direct radiative recombination in the host crystal has been derived in a classical paper by Hall.[4] In a nondegenerate semiconductor, the rate at which electrons and holes disappear by this process is given by

$$R = B_r(np - n_i^2) \tag{1}$$

where $n = n_o + \Delta n$, $p = p_o + \Delta p$; n_i is the intrinsic carrier density; Δn and Δp are excess electron and hole density respectively. For large injection case, $\Delta n = \Delta p >> n_o, p_o$, Eq. (1) reduces to

$$R \cong B_r \Delta n \Delta p \tag{2}$$

Here B_r is the radiative capture rate which can be evaluated theoretically by setting the equilibrium rate of radiative recombination equal to the total

amount of the black body radiation absorbed by the crystal due to direct band to band transition process. This has been derived by Hall[4] and is given by

$$B_r = 0.58 \times 10^{-12} (\varepsilon_s)^{\frac{1}{2}} \left(\frac{m_o}{m_e + m_h}\right)^{\frac{3}{2}} \left(1 + \frac{m_o}{m_e} + \frac{m_o}{m_h}\right) \left(\frac{300}{T}\right)^{\frac{3}{2}} E_g^{\,2} \ \text{cm}^3/\text{sec} \qquad (3)$$

where m_o is the free electron mass; m_e and m_h are the electron and hole effective masses respectively; ε_s denotes the dielectric constant of the semiconductor, and E_g is the band gap of the semiconductor.

Eq. (3) predicts that for direct band to band radiative recombination the capture rate is inversely proportional to $T^{3/2}$, assuming that other parameters in Eq. (3) are insensitive to temperature.

The excess carrier lifetimes for band to band radiative recombination under large injection condition can be defined in terms of the recombination rate given by Eq. (2). Thus

$$\tau_r = \tau_n = \tau_p = \frac{\Delta n}{R} = \frac{\Delta p}{R} = \frac{1}{B_r \Delta p} = \frac{1}{B_r \Delta n} \qquad (4)$$

where τ_r is the radiative recombination lifetime; τ_n and τ_p are electron and hole lifetimes respectively.

We shall employ the result of Eq. (4) in our PME and PC theory to be discussed next.

(B) Photomagnetoelectric (PME) and photoconductive (PC) theory for the band to band radiative recombination

It has been shown that oxygen impurity introduces a deep donor level with neutral charge state in GaAs.[5] At low temperatures our experimental results indicate that the oxygen donor level is neither acting as an effective recombination center nor as a trapping center. As a result, it is assumed that the band to band radiative recombination process is the dominant mechanism responsible for the recombination of electrons and holes in O -doped GaAs at low temperatures. This is indeed the case as will be shown later in this paper .

Since our experimental conditions for the PME and PC measurements in O -doped GaAs are such that the excess carrier density Δn and Δp are always greater than the thermal equilibrium carrier density n_o (at 4.2°K

and 20.8°K), the derivation of the PME and PC theory will be made under the assumption of large-injection conditions. The dependence of carrier lifetimes on the injected-carrier density is given by Eq. (4). A generalized expression for the PME short circuit current per unit magnetic flux density, B, for arbitrary injection and trapping conditions has been given by Li and Huang.[6] If we set $\Gamma = 1$ (i.e., $\tau_n = \tau_p$, no trapping), $\kappa = B_r^{-1}$ and $\beta = -1$ in Eq. (7) of reference [6] and assuming that the electron and hole mobility ratio, b, is much greater than unity in GaAs, we obtain an expression for the PME short circuit current for the radiative recombination case. This can be written as

$$I_{PME}/B = \frac{1}{6} \left(\frac{B_r}{q\mu_n}\right) \Delta G^2 \tag{5}$$

where I_{PME} is the PME short circuit current per unit sample width and B is the magnetic flux density. The capture rate B_r is defined by Eq. (3), μ_n is the electron mobility and ΔG is the photoconductance per unit sample length-to-width ratio. The simple result by Eq. (5) is rather important, since it provides a direct way of determining the capture rate from three measurable quantities I_{PME}/B, ΔG and μ_n. It also provides a direct correlation between the two measurable quantities I_{PME} and ΔG.

For large injection case, the PME short circuit current per unit magnetic flux density is related to the carrier lifetime and the photoconductance by the following expression[6]

$$I_{PME}/B = \left(\frac{2D_p}{\tau_n}\right)^{\frac{1}{2}} \Delta G \tag{6}$$

By comparing Eqs. (5) and (6) we obtain the electron and hole lifetimes for radiative recombination case:

$$\tau_n = \tau_p = 72\, D_p \left(\frac{q\mu_n}{B_r \Delta G}\right)^2 \tag{7}$$

The result of Eq. (7) shows that the electron and holes lifetimes for band to band radiative recombination are inversely proportional to the square of the photoconductance under large injection case.

The relation between the photoconductance and the injected excess carrier density at the illuminated surface of the sample, Δn_s, can also

be derived from Eq. (3a) of reference [6] for the present case. The results are

$$\Delta G = (2q\mu_n)\left(\frac{3D}{B_r}\right)^{\frac{1}{2}} \Delta n_s^{\frac{1}{2}} \qquad (8)$$

which shows a quadratic dependence of Δn_s on ΔG.

III. Results and Analyses

The photo-Hall, photomagnetoelectric and photoconductive experiments in O -doped n-type GaAs samples have been conducted at T = 4.2°K and 20.8°K respectively [7]. The electron density in these samples measured at 300°K varies from 10^{14} to 10^{15} cm^{-3}. The experimental details are similar to those described in reference [8] and will not be repeated here. The electron mobility μ_n is 3500 cm^2/V-sec at 300°K.

The result of the photo-Hall mobility data is displayed in Fig. 1, for T = 4.2°K and 20.8°K. Note that the electron mobility is near constant for $\Delta G \leq 10^{-5}$ mho but increases with increasing light intensity. The present result shows that μ_n varies with $\Delta G^{0.2}$ for $\Delta G > 10^{-5}$ mho.

A plot of I_{PME}/B versus ΔG for T = 4.2°K and 20.8°K is shown in Fig. 2. From this plot it is found that I_{PME}/B varies with ΔG^2, in good agreement with the prediction given by Eq. (5). By using Eq. (5) and data in Figs. 1 and 2, the capture rates for band to band radiative recombination is calculated for O -doped n-type GaAs. The results yield

$$B_r = 1.15 \times 10^{-8} \text{ cm}^3/\text{sec at T} = 20.8°\text{K}$$
$$B_r = 1.23 \times 10^{-7} \text{ cm}^3/\text{sec at } 4.2°\text{K}$$

To compare the above experimental values of the capture rates with those predicted by the Hall's direct radiative recombination formula, we use Eq. (3) to compute B_r for GaAs at 4.2°K and 20.8°K, the results are

$$B_r = 1.07 \times 10^{-8} \text{ cm}^3/\text{sec at } 20.8°\text{K}$$
$$B_r = 1.18 \times 10^{-7} \text{ cm}^3/\text{sec at } 4.2°\text{K}$$

Here $m_e/m_o = 0.068$, $m_h/m_o = 0.5$, and $E_g = 1.51$ eV have been used in Eq. (3) to compute B_r for GaAs.

The above result shows that the values of B_r determined from the present PME and PC measurements are in excellent agreement with those computed from Hall's direct radiative recombination formula, Eq. (3).

The electron and hole lifetimes can be determined from Fig. 2 and Eq. (6). The result is also plotted in Fig. 3. Note that for $\Delta G \lesssim 10^{-5}$ mho, τ is proportional to ΔG^{-2} in accord with the prediction given by Eq. (7). However, for $\Delta G > 10^{-5}$ mho, τ varies with $\Delta G^{-1.6}$. The change in slope of τ versus ΔG plot is due to the fact that μ_n also changes with ΔG for high light level (i.e., $\mu_n \propto \Delta G^{0.2}$ for $\Delta G > 10^{-5}$ mho). Estimation of excess carrier density from Eq. (8) indicates that $\Delta n = 2.5 \times 10^{10}$ cm^{-3} at 20.8°K and 2.6×10^{12} cm^{-3} at 4.2°K for $\Delta G = 10^{-5}$ mho. These values are much much higher than the equilibrium electron densities at both temperatures. Thus the assumption of high injection case is justified for the present case.

In conclusion, we have shown that the photoinjected excess carrier recombination process in O -doped n-type GaAs at 20.8°K and 4.2°K is dominated by the band to band radiative recombination. The deep level oxygen impurities in GaAs are neither acting as recombination centers nor as trapping; centers for the excess carriers. The radiative capture rates can be determined readily from concurrent measurements of the PME short circuit current and the photoconductance of the samples.

REFERENCES

1. R. Braunstein, Phys. Rev. 99, 1892 (1955).
2. S. Mayburg, Solid State Electronics, 2, 195 (1961).
3. T. Kinsel and I. Fudman, Solid State Electronics, 8, 797 (1965).
4. R. N. Hall, Proc. Inst. Elec. Engr., 106B, Suppl. 17, 983 (1960).
5. S. M. Sze and J. C. Irvin, Solid State Electronics, 11, 599 (1968).
6. S. S. Li and C. I. Huang, J. Appl. Phys., 43, 1757 (1972).
7. C. I. Huang and S. S. Li, Solid State Electronics, to be published (1973); the oxygen concentration was found to be varying from 2×10^{15} to 5×10^{15} cm^{-3} for several O_2-doped GaAs sampl as determined from C-V measurements.
8. S. S. Li and C. I. Huang, Phys. Rev., 4, 4633 (1971).

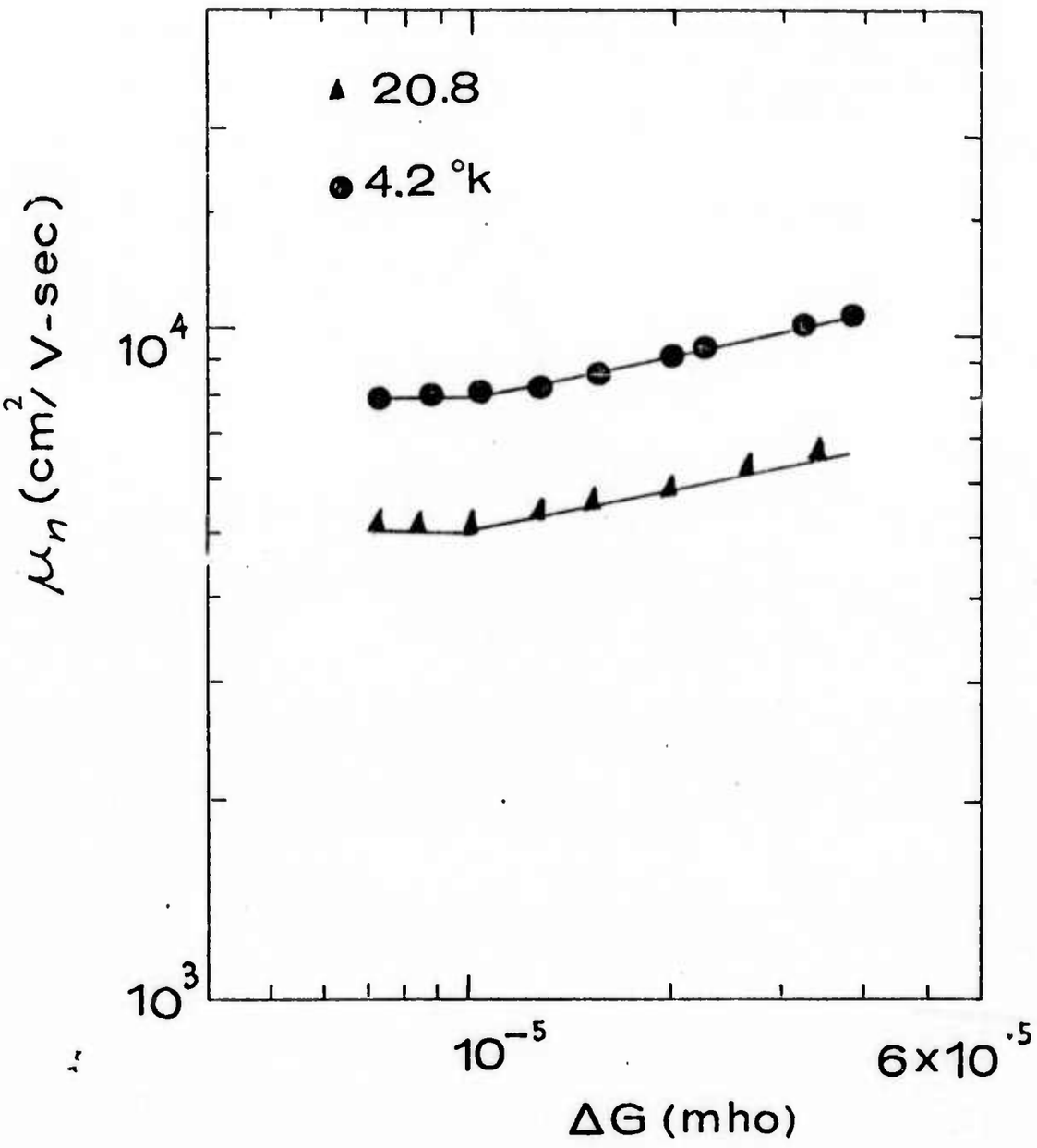

Fig. 1 The photo-Hall mobility versus photoconductance for O_2-doped n-type GaAs measured at T = 20.8°K and 4.2°K.

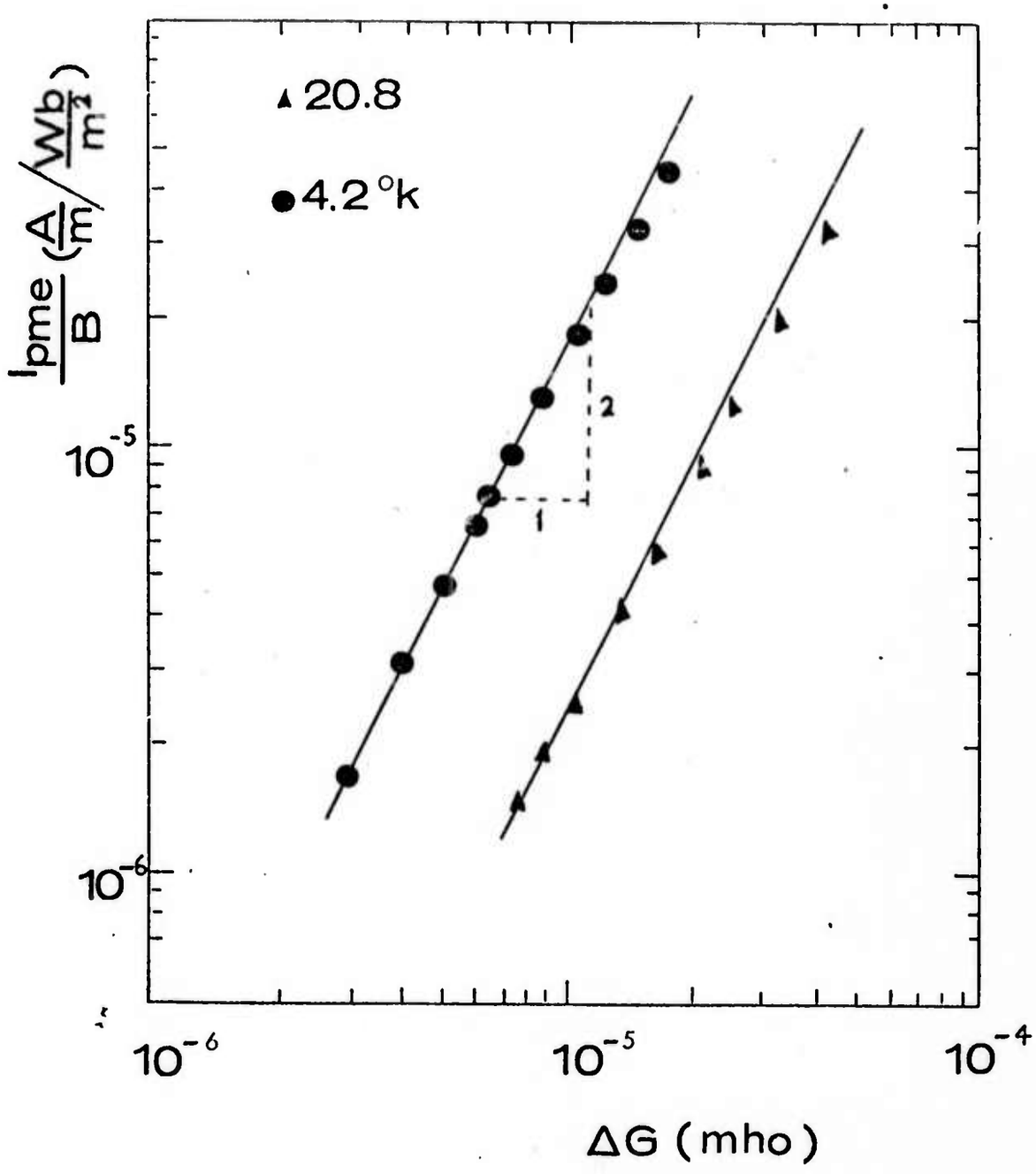

Fig. 2 The PME short-circuit current per unit sample width per unit magnetic flux density, I_{PME}/B, versus photocnductance ΔG for O_2-doped GaAs samples at 20.8°K and 4.2°K.

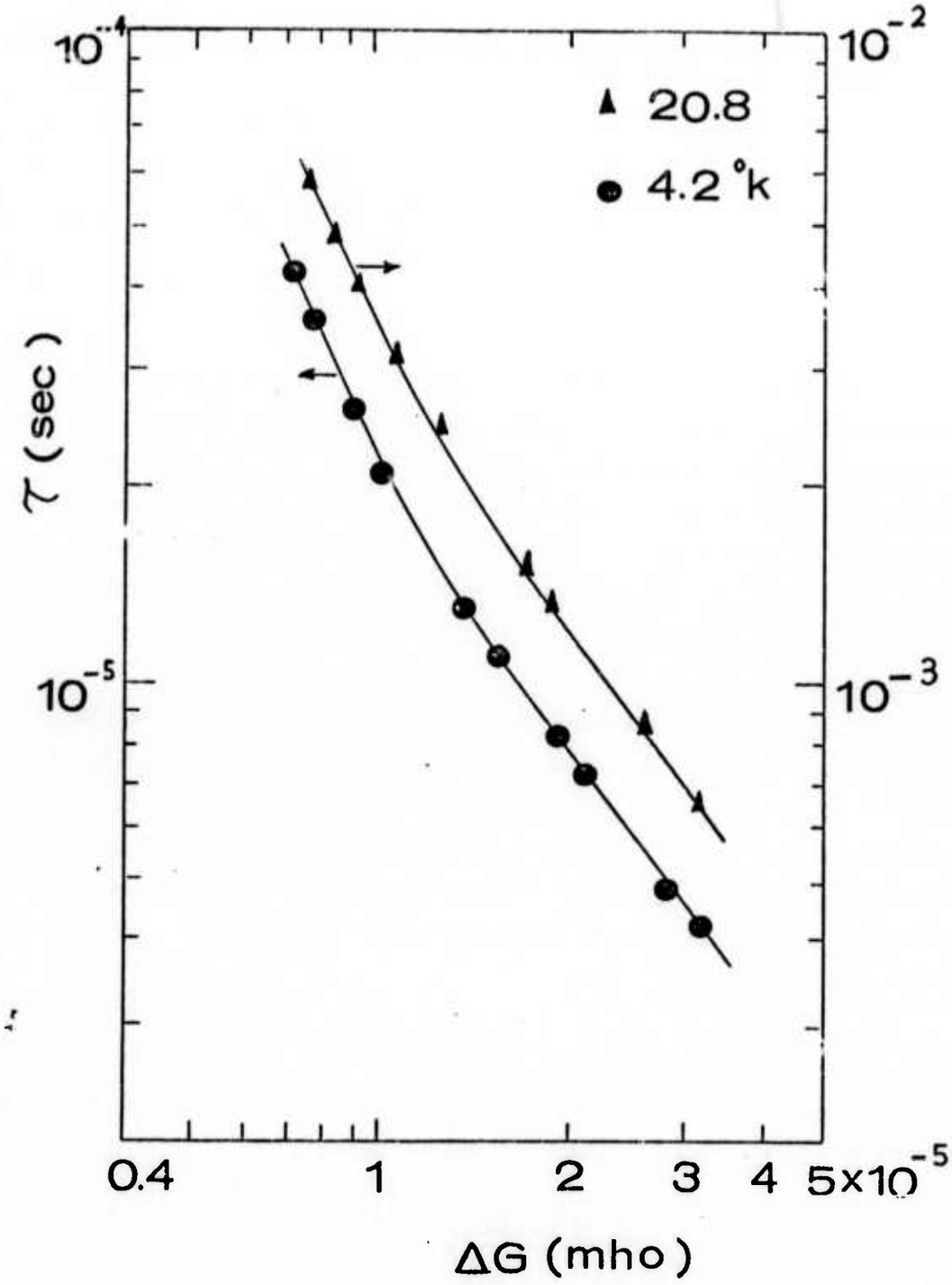

Fig. 3 The PME and PC lifetimes versus photoconductance ΔG for O_2-doped GaAs for T = 20.8°K and 4.2°K. Here $\tau = \tau_n = \tau_p$.

IV. Injection Dependence of the Excess Carrier Lifetimes in Cr-doped n-type GaAs (C. I. Huang and S. S. Li)

This short communication is an extension of our previous work[1] on the study of recombination and trapping processes in Cr-doped GaAs, employing PME and PC methods. The main purpose of this report is to illustrate both theoretically and experimentally the injection dependence of the excess carrier lifetimes in Cr-doped n-type GaAs. In addition to the previously reported photomagnetoelectric (PME) and photoconductive (PC) measurements in the high and intermediate injection ranges[1] we have extended the present experiments to cover the lower injection range by using AC method. The result of the PME short circuit current versus photoconductance is plotted in Fig. 1 for T = 300°K. Two linear injection ranges are observed respectively at high and low injection ranges, which are connected by a nonlinear intermediate injection range. This result can be interpreted in terms of the generalized PME expression derived in our previous paper.[1]

$$I_{PME} = 2q\mu_p(1+b)\,BF D_p\left[\frac{(2+\beta)^2}{4(2-\beta)D_p\Gamma K}\right]^{\left(\frac{1}{2+\beta}\right)}\left(\frac{\Delta G}{q\mu_n}\right)^{\frac{2}{2+\beta}} \qquad (1)$$

The generalized PME lifetime, equivalent to the above expression, can be derived from reference (1) and is given by

$$\tau_a = \frac{1}{2D_p\Gamma^2}\left[\frac{(2+\beta)^2}{4(2-\beta)D_p\Gamma K}\right]^{\left(\frac{-2}{2+\beta}\right)}\left(\frac{\Delta G}{q\mu_m}\right)^{\frac{2\beta}{2+\beta}} \qquad (2)$$

A plot of τ_a (deduced from Fig. 1) versus ΔG is displayed in Fig. 2. The results shown in Fig. 1 and 2 can be interpreted as follows. At high injection range (I), $\beta = 0$, $\Gamma = 1$, $\tau_a = \tau_n = \tau_p$, the PME short

circuit current, I_{PME}, is linearly proportional to ΔG and the lifetime is independent of injection (i.e. τ_n is constant). In the intermediate injection range (II), $\beta = -\frac{1}{3}$, $\tau_p = \Gamma\tau_n$, the I_{PME} varies with $\Delta G^{1.2}$ and the PME lifetime τ_a is proportional to $\Delta G^{1.4}$. In the lower injection range (III), another linear region for I_{PME} versus ΔG was observed. In this region, $\beta = 0$, $2\tau_a = \tau_n = \tau_p$, the excess carrier lifetime is independent of injected carrier density. The theoretical calculation of the dependence of carrier lifetimes on the excess carrier density given by Agraz and Li[3] has been clearly demonstrated experimentally in this paper for the Cr-doped GaAs.

References

1. S. S. Li and C. I. Huang, J. Appl. Phys. 43, 1757 (1972).

2. W. Shockley and W. T. Read, Jr., Phys. Rev. 87, 835 (1952).

3. J. Agraz-Guerena and S. S. Li, Phys. Rev. B2, 4966 (1970).

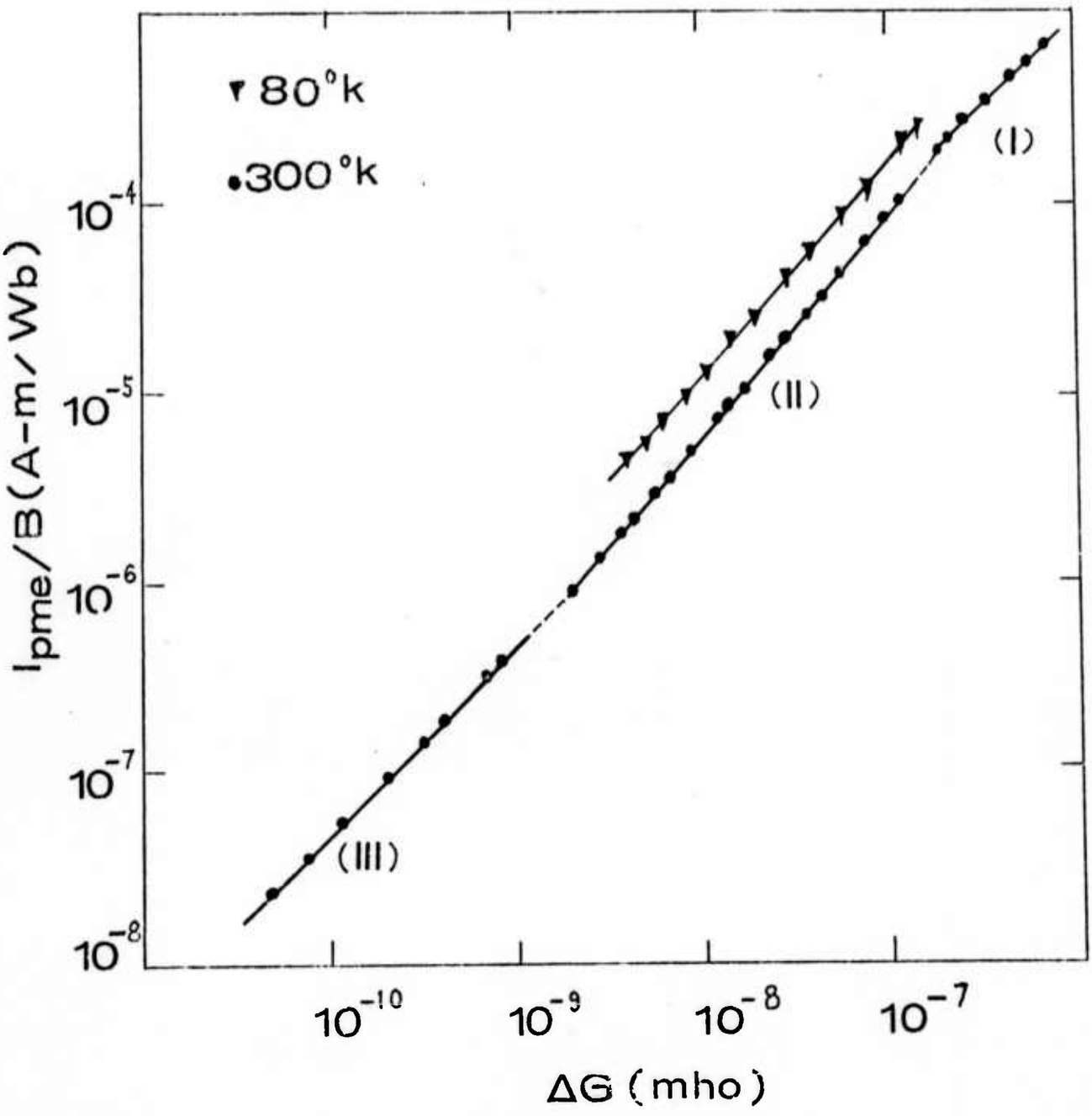

Fig. 1 The PME short-circuit current per unit width of sample per unit magnetic flux density, I_{PME}/B, vs. photoconductance ΔG for samples S-1 and S-2 at 80 and 300°K.

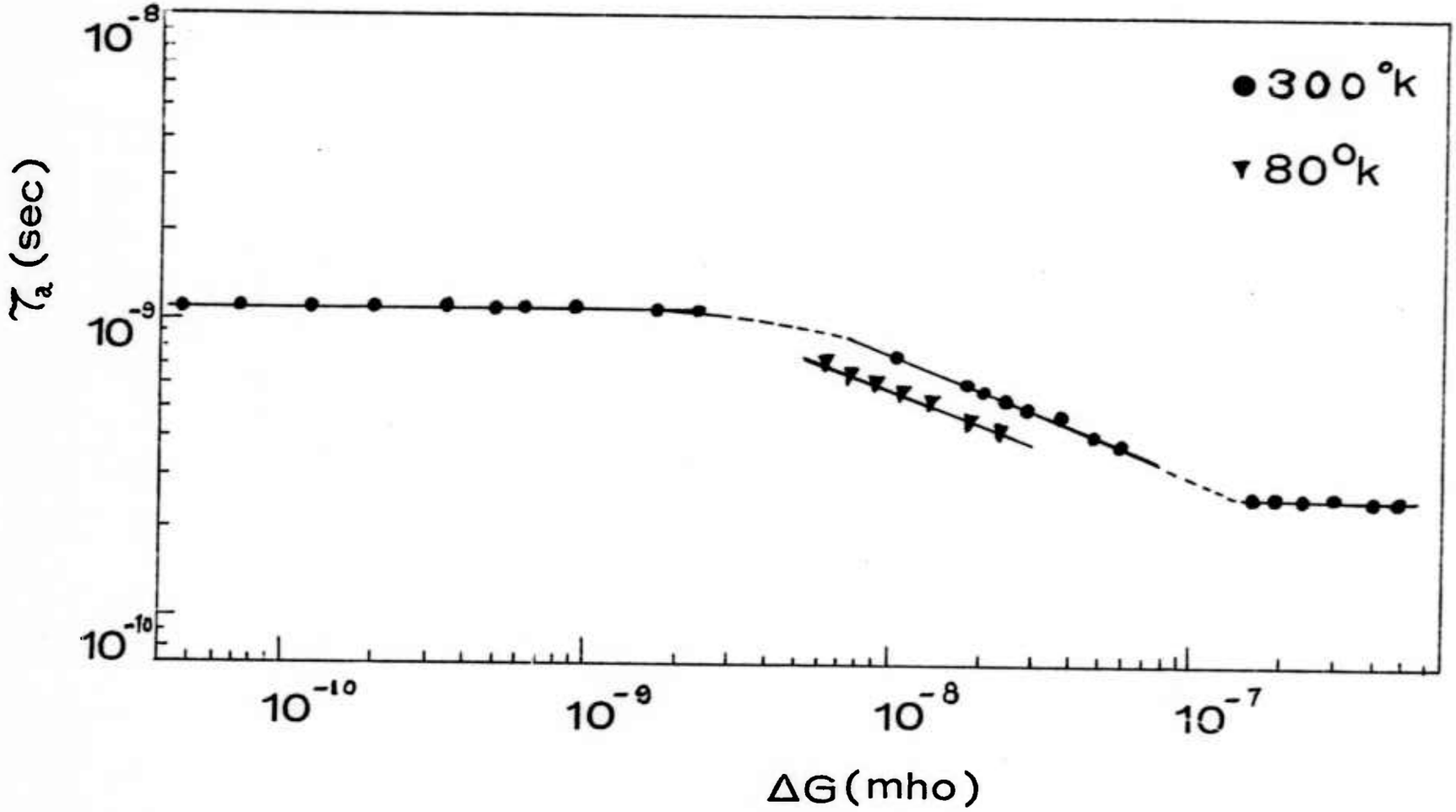

Fig. 2 The PME effective lifetime, τ_a, the electron lifetime, τ_n, and the hole lifetime, τ_p, vs. ΔG for sample S-2 at 80 and 300°K. The data shown in region (I) is for sample S-1 at 300°K

V. Reverse I-V Characteristics in Au-GaAs Schottky Diode in the Presence of Interfacial Layer (C. I. Huang and S. S. Li)

It has been shown that the thickness of the interfacial layer between Au and GaAs may vary from 5 to 30 Å under ordinary laboratory fabrication conditions.[1] It is true that this interfacial layer becomes electrically transparent under high electric field. However, the current-voltage relation at very low bias voltage becomes very complex in the presence of interfacial layers. Simons[2] derived a formula for the electric tunneling effect through a potential barrier of arbitrary shape existing in a thin insulating film.

For very low applied voltage, the tunneling resistivity is constant.[2,3] Thus the interfacial layer in a Schottky diode can be treated as a high resistance series resistor. Its resistance value depends on the thickness of the layer, equivalent barrier height and the dielectric constant of the layer.[2,3]

Au-GaAs Schottky doides were fabricated by evaporating Au onto a chemically etched Cr-doped n-type GaAs wafer with the carrier concentration of $10^{14} \sim 10^{15}$ cm^{-3} (at 300°K). The depletion layer width for these diodes is in the order of 100 μm at zero bias condition. Accordingly, the most probable mechanism of electron transport is by thermionic emission. Thus, including the dipole layer[4] and the barrier lowering effects,[5] the reverse I-V relation can be expressed by

$$J = A^*T^2 \exp\left\{\frac{q}{kT}\left[-\phi_{bo} + \left(\frac{q\mathcal{E}}{4\pi\epsilon_s}\right)^{1/2} + \alpha\mathcal{E}\right]\right\}\left[\exp\left(\frac{qV}{mkT}\right) - 1\right] \qquad (1)$$

where m is a voltage dividing factor and is essentially a function of interfacial layer resistivity; the rest of the parameters have the conventional meaning as defined in Refs. 4 and 5. At very low reverse bias voltage, Eq. (1) becomes

$$J = A^*T^2 \exp\left(\frac{-q\phi_{bo}}{kT}\right)\left(\frac{q}{kT} \times \frac{V}{m}\right) \qquad (2)$$

which shows that Au-GaAs contact is ohmic under very low bias condition (i.e., a linear relation between J and V).

The reverse I-V relation of a typical Au-GaAs Schottky diode is shown in Fig. 1. Experimental data is shown by the circles while the solid line represents a theoretical fit by Eq. (1), with the following parameters:

$N_D = 2.7 \times 10^{14}$ cm^{-3} $\quad$ $m = 9$

$A^* = 4.4$ $amp/cm^2/°K^2$ $\quad$ $\alpha = 1.44 \times 10^{-6}$ cm

$\phi_{bo} = 0.85$ eV

For $V > -0.15V$, the term $[\exp(\frac{qV}{mkT})-1]$ dominates the behavior of reverse current I; this is due to the existence of an interfacial layer. Instead of solving the complicated tunneling problem we have used the empirical parameter m as an adjustable parameter for estimating the intimacy of metal-semiconductor contact. For metal-silicide Schottky diodes, the problem of interfacial layer *does* not exist and m value is unity.[4] For comparison, the prediction with m = 1 is also given in Fig. 1.

In the range of higher reverse bias voltages, the interfacial layer becomes transparent to the electron flow and the barrier lowering mechanisms dominate the I-V characteristics. The value of $\alpha = 1.44 \times 10^{-6}$ cm for our device is higher than that of metal-silicide Schottky diodes.[4] This indicates that the dipole layer effect in our device is more prominent than those reported in reference 4. The existence of the deep level impurity (Cr) might enhance this effect.

In summary, we have shown that the existence of an interfacial layer in a Au-GaAs Schottky diode can be revealed by measuring the I-V characteristics at very low reverse bias voltages.

References

1. B. R. Pruniaux and A. C. Adams, J. Appl. Phys. 43, 1980(1972).

2. J. G. Simons, J. Appl. Phys., 34, 1793 (1963).

3. J. Unterkofler, J. Appl. Phys., 34, 3145 (1963).

4. J. M. Andrews and M. P. Lepselter, Solid State Electron, 13, 1011 (1970).

5. S. M. Sze, Physics of Semiconductor Devices, Wiley-Interscience, New York (1969).

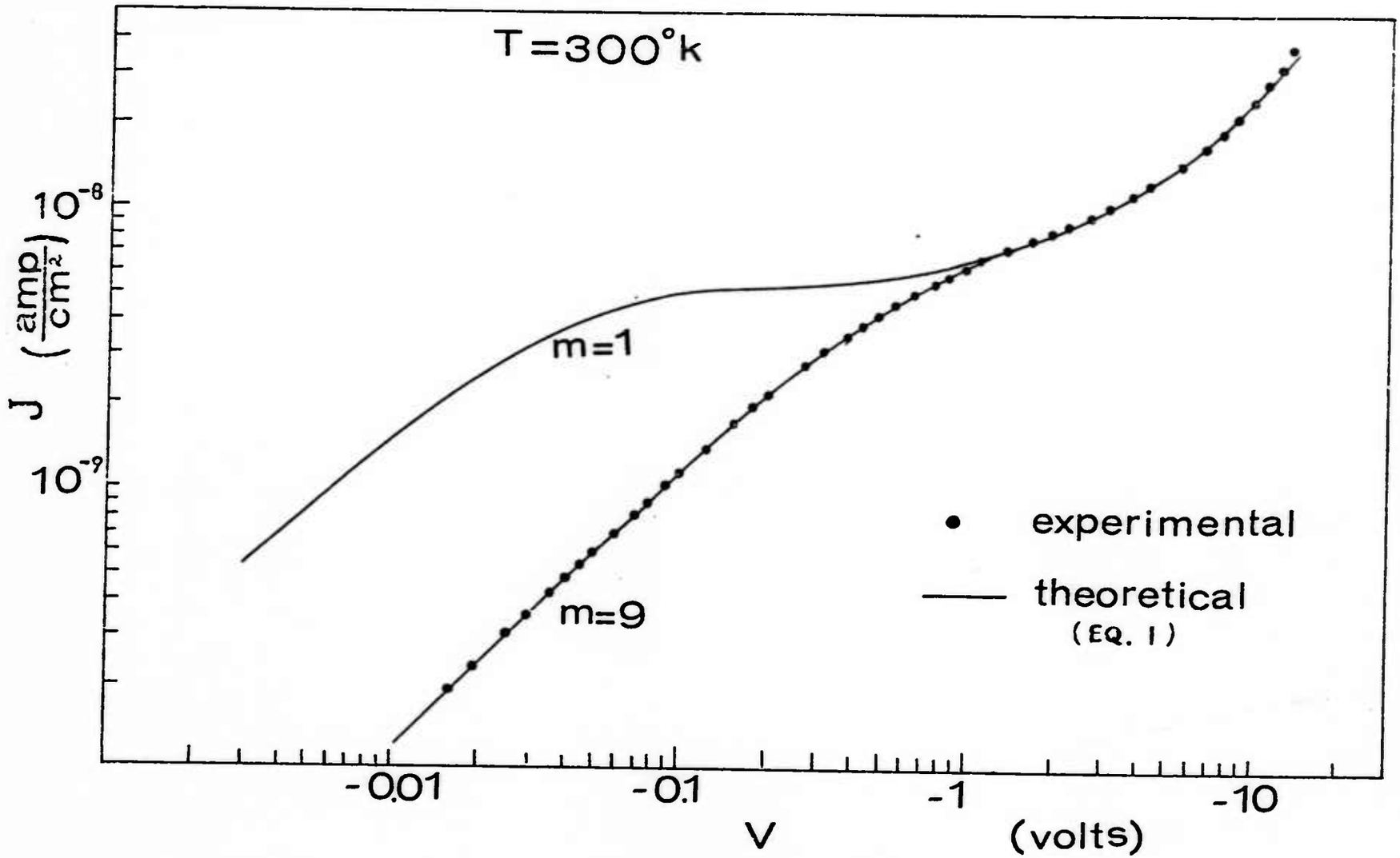

Fig. 1

Reverse current-voltage characteristics of Au-GaAs (n-type) Schottky diode (D-17) at 300°K.

VI. Discussion

This first report has dealt mainly with properties of semiconductors that bear on the operation of photodetectors and that play a role in the modeling of various semiconductor devices.

Research now in progress and nearing completion will supply much of the content of the next report in the series. A unification of nearly all of the circuit models previously proposed for bipolar and MOS transistors will be suggested that will ease several problems now existing in the computer simulation and design of semiconductor circuits. The proposed unification will include the effects of exposure to radiation environments. A thorough study of the noise spectrum of irradiated junction field-effect transistors will be presented, as will inferences concerning the design of these devices. From our research concerning carrier-domain devices, we will describe some fundamental bounds related to design and give the details of devices we have fabricated that yield 4-quadrant multiplication and the realization of an arc-sine function between input and output variables.

Additionally, our next report will continue to describe material parameters that bear on the design of semiconductor devices and on characterizations used in the computer-aided design of semiconductor circuits.